UCID-18158

Lawrence Livermore Laboratory

Parametric Studies of Tandem Mirror Reactors

G. A. Carlson, B. M. Boghosian,
*J. H. Fink, J. O. Myall, W. S. Neef Jr.

April 26, 1979

Prepared for the Tandem Mirror Review at Department of Energy, Washington D.C.

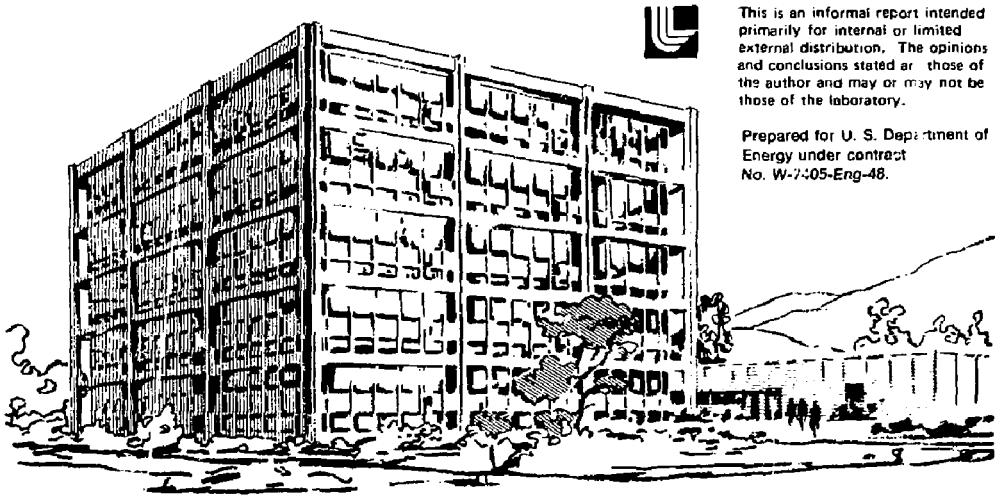

Prepared for U. S. Department of Energy under contract No. W-7405-Eng-48.

*on loan from Westinghouse

PARAMETRIC STUDIES OF TANDEM MIRROR REACTORS

By

G. A. Carlson, B. M. Boghosian,
J. H. Fink, J. O. Myall, W. S. Neef Jr.

Executive Summary

This report, along with its companion, An Improved Tandem Mirror Reactor,[1] discusses the recent progress and present status of our tandem mirror reactor studies. This report presents the detailed results of parametric studies up to, but not including, the very new idea involving thermal barriers, which are discussed in Ref. 1.

The parametric studies were carried out with an analytic zero-dimensional physics model, which has been in a continual state of development since first presented in the TMX Proposal.[2] The development has resulted in more accurate calculations and a more versatile computational tool. A recent major sophistication has been the addition of a controller program for automatic optimization.

The major goal of our tandem mirror reactor studies since the publication of our preliminary design report[3] has been to improve reactor performance, while at the same time lowering the level of required technology (principally neutral beams and magnets). Ideas which have been investigated are the addition of "A" cells, direct electron heating in the central cell, direct electron heating in the plugs, and thermal barriers to insulate the plug electrons from the central cell electrons. The first three ideas are discussed in this report.

"A" cells are auxiliary plasma cells placed at each end of the tandem mirror, outside the plug cells. The purpose of the "A" cell is to reduce the outward potential drop of the plug plasma and thus improve the confinement of

the plug plasma. The required injection power for the "A" cell can be very small, and a net benefit can be realized either as a reduction in plug injection energy, or improved performance, or both. An additional benefit from "A" cells is that minimum-B "A" cells may MHD stabilize the entire tandem mirror system, allowing the use of simple mirror plug cells. For equal on-axis field strengths, simple mirror plugs can be designed with lower maximum fields than minimum-B plugs.

Direct electron heating in the central cell allows a further reduction in injection energy and results in a further improvement in performance. Electron cyclotron heating (ECH) in the central cell could be done at the microwave frequency of gyrotrons under development (110 GHz).

Direct electron heating in the plugs by ECH would require the development of higher frequency gyrotrons, but would result in another reduction in required injection energy and another improvement in performance. The improvements are due to the significantly higher electron temperature which is established in the plug.

The fourth idea, the thermal barrier concept, is discussed in detail in Ref. 1. Basically, the concept involves the maintenance of a mirror cell with depressed plasma potential between the central cell and plug. This depression in the potential serves as an electron thermal barrier between the central cell and plug. Electron heating in the plug can then result in a very much higher electron temperature there, and a large improvement in tandem performance. The effect of the thermal barrier is so strong that large relaxations of technology can be made. A reduced plug magnetic field and plasma density allows the use of ECH heating in the range 55 to 110 GHz in the plug region.

Table 1 gives a short list of parameters for three different tandem mirror reactors. The first column is the case previously discussed in Ref. 4. This unoptimized design used "A" cells and direct electron heating in the central cell. We see that the injection energy is reduced from the 1200 keV specified for our preliminary design,[3] but the plug magnetic field strength is very high. (The lower value for B_{max} refers to a simple mirror plug, i.e., MHD stabilization by the "A" cell; the higher value refers to a Yin-Yang plug.)

	"A" cells and central cell electron heating	"A" cells and plug electron heating	Thermal Barriers
E_{inj}	600 keV	350	200
B_{max}	19 or 21 T	15 or 17	12
$P_{neutral\ beam}$	80 MW	42	10
$P_{electron\ heating}$	130 MW	250	57
P_{fusion}	2100 MW	3000	1500
L_c	240 m	320	50
r_{fw}	1.9 m	0.9	1.1
Q	10	10	23
Γ	0.6 MW/m^2	1.3	3.6*

* This value can always be reduced by increasing the first wall radius if such proves to be cost effective from the wall lifetime point of view.

Table 1. Three Tandem Mirror Reactors.

The second column is an optimized design with "A" cells and direct electron heating in the plugs. This case is discussed more fully in this report. Compared to the first column, we see a significant reduction in neutral beam energy and maximum magnetic field strength. The plasma Q is the same for the two cases, but the first wall neutron loading Γ is more than twice as high for the second case. However, the reduced first wall radius for the second case means that the fusion power density volume-averaged over the annular central cell does not increase as the ratio of Γ's, but rather as $(1.3(0.9 + 0.5\ t))/(0.6(1.9 + 0.5\ t))$ where t is the thickness of the central cell annulus (blanket, shield, and magnet). Taking t = 2.0 m as typical, we find the ratio to be 1.4, still greater than unity.

The third column is a preliminary, unoptimized design incorporating the thermal barrier concept. This case is discussed more fully in Ref. 1. The improvements over the first two cases are striking. The neutral beam injection energy is reduced to 200 keV, and only 10 MW of beam power is required. The maximum magnetic field is reduced to 12 T. Q is increased to 23 and Γ to 3.6 MW/m^2. Of course, this wall loading can always be reduced by increasing the first wall radius, if such proves to be cost effective from the wall lifetime point of view. Doubling the first wall radius (halving the first wall loading) would increase the material volume of the annular central cell ($\sim$ 2 m thickness) by a factor of 1.5. The reactor is attractively dimensioned--the central cell has a first wall radius of 1.1 m and a length of 50 m. Clearly, the thermal barrier concept can result in a superior reactor.

Our future reactor studies must thoroughly investigate the details for the thermal barrier concept. Our analytic physics model must undergo a major modification to include thermal barriers. Then we will be able to do more accurate calculations and begin to optimize a design. Equally important, we

must investigate fully the technology requirements of the thermal barrier, as discussed briefly in Ref. 1. If these studies show that the parameters of Table 1, third column can be achieved or bettered, we will have achieved our goal of significant tandem mirror performance improvement with reduced technology requirements.

Introduction

The objectives of the tandem mirror reactor parametric studies are to develop a more thorough understanding of reactor scaling, to assess the potential of new ideas, and to specify consistent parameter sets for attractive reactor cases. This report presents the results of the parametric studies up to, but not including, the very new ideas of Grant Logan, David Baldwin, and Ken Fowler involving thermal barriers.[1] Continued development of the tandem mirror physics model has resulted in more accurate calculations and a more versatile computational tool. The results are presented in a general power balance vs power density format which permits after-the-fact tradeoff evaluations. New ideas, which have been thoroughly investigated, are the addition of "A" cells and the optimal use of direct electron heating. "A" cells, first proposed by Logan[4] and later considered at the University of Wisconsin,[5] are auxiliary plasma cells placed at the ends of the tandem mirror. The purpose of the "A" cell is to contain a plasma about equal in density to that in the central cell, so that the outward potential drop of the plug plasma is reduced to approximately equal the inward potential drop. The resulting confinement of the plug plasma is improved, and, as will be shown, the overall power balance improves. Direct electron heating was considered briefly in our preliminary TMR design report,[3] but not thoroughly investigated. We have now considered the optimal amount and location of direct electron heating. In this report, we

summarize the predicted performance of tandem mirror reactors which do not incorporate thermal barriers and specify the technology developments necessary for such reactors. In the next few months, we will consider the use of thermal barriers which promise further improvements in TMR performance, along with further reductions in technology requirements.(1)

Physics Model Development

The analytic zero-dimensional physics model for the tandem mirror reactor was first presented in the TMX Proposal(2) and was discussed further in Ref. 3. Since then, a number of minor corrections and improvements have been made, and several major modifications have been incorporated. One of these is a much-improved analytic model for plug plasma confinement. This model, developed by Grant Logan and Marvin Rensink, has been shown to be in good agreement with Fokker-Planck calculations over a considerable range of electron drag vs ion scattering.(6)

Another important addition to the physics model is an option to include "A" cells on the tandem mirror. Given the injection energy, mirror ratio, and β for the "A" cell, this option uses the Logan/Rensink plug model to calculate the required magnetic field strength and injection power for the "A" cell. The overall plasma Q calculation is corrected to include the "A" cell power requirement.

Another addition to the physics model is an option to ensure DCLC stability of the plug (and/or the "A" cell) by the gradient stabilization method. This option uses results from Pearlstein(7) relating plug size, magnetic field strength, energy, and β. In the physics model, the plug β is adjusted to give marginal stability. Because of the preliminary nature of this treatment of DCLC stability, this option was not exercised for the majority of the cases reported here. We do, however, give example results.

A further refinement to the physics model is the discrimination of trapped (plug) and passing (central cell) electrons in the energy balance equations. Whereas previous physics modeling had assigned only one temperature to all electrons in the reactor, the new model allows for the trapped and passing electrons to have different temperatures by performing a separate energy balance on each of these two species. Of course, to do this, it is necessary to have an expression for the thermal conductivity power transfer between the trapped and passing electrons; the theoretical development of such an expression was done by Logan, Baldwin, and Fowler.[8] As we will see, direct electron heating in the plugs can result in a large and beneficial electron temperature difference between the plugs and central cell.

If wall loading and fusion power are constrained to particular values, it is often desired to maximize Q with respect to both the central cell magnetic field strength and the electron heating fraction. As this process of two-dimensional transcendental function maximization can be time consuming if done by hand, a controller code was developed for this purpose. The controller uses the simplex method for function optimization.[9] This algorithm has the virtues of requiring relatively few evaluations of Q (controllee runs) per step, and allows for easy generalization to higher dimensional optimization. Thus, if it were desired to optimize with respect to, say, plug mirror ratio as well, the controller would need only very minor modifications. Similar minor modifications could be made to constrain different quantities while Q is maximized. We have calculated many of the results in this report without using the controller because we wanted to study the trends of parameter variation, not just the optimum cases. We do, however, give some results generated by the controller.

It must be emphasized that the tandem mirror physics model has been, and will continue to be, the heart of our parametric studies, and that the model is in a continual state of development. A major revision is now underway to incorporate the new ideas of thermal barriers to further enhance the favorable high temperature of trapped electrons in the plugs. Future revisions are to be expected following new theoretical or experimental insights into tandem mirror behavior. The goal of the parametric studies effort is to maintain an up-to-date model for the treatment of tandem mirror physics in a parameter range appropriate for a reactor.

Some Parameter Choices

To place reasonable limits on the scope of our parametric studies, we held some parameters constant for the majority of the calculations reported here.

We constrained the total fusion power to be 3000 MW. Given typical component efficiencies and a plasma Q high enough to yield a low recirculating power fraction, such a reactor will produce ~1000 MWe net output.

We took the vacuum magnetic field strength at the center of the plug to be 10.6 T and the vacuum mirror ratio to be 1.2, resulting in an on-axis mirror field of 12.7 T. The mirror ratio was chosen based on the expectation (not yet conclusively demonstrated) that a minimum-B plug coil with this axial well can be designed with sufficient radial well depth to provide MHD stabilization for the entire tandem mirror system. The two magnetic field quantities given above are the important ones for the physics model, but the maximum magnetic field strength at the conductor is of more importance to magnet technology. We define magnet efficiency as the ratio of on-axis mirror field to maximum magnetic field at the conductor. Magnet efficiency is a function of magnet configuration and conductor bundle size and shape. We have found that magnet

efficiencies of about 75% are achievable with minimum-B Yin Yang plug coils, resulting in a 17 T maximum magnetic field for the case chosen above. The incorporaton of "A" cells into the tandem mirror design opens up the possibility that MHD stabilization can be provided by minimum-B "A" cell magnets, which are of lower field strength than the plug coils, and that the plugs can be non minimum-B, i.e., simple solenoidal mirrors. We are still in the process of evaluating the MHD stability of such a design, but if feasible, it will reduce the maximum magnetic field strength because of the higher efficiency of simple solenoidal mirrors. Our calculations indicate an achievable magnet efficiency of about 84% for simple mirror plug coils, resulting in a 15 T maximum magnetic field for the case chosen above. Thus, the plug magnet parameters chosen for the calculations reported here imply maximum magnetic field strengths in the range of 15 to 17 T, depending on the plug/"A" cell magnet configuration. We will also report briefly on the effects of lower plug magnet field strengths.

We took the plug plasma β to be 1.0 and used the "short-fat" approximation[3] which predicts a plasma magnetic field strength of $B_{vac}(1 - \beta/2)$, i.e., a field depression of 50%. In cases where we exercised the DCLC stability option, the plug β was allowed to change to satisfy the marginal stability criterion.

We took the central cell plasma β to be 0.7 and used the "long-thin" approximation[3] which predicts a plasma magnetic field strength of $B_{vac}\sqrt{1-\beta}$, i.e., a field depression of 45%. The achievable central cell β is a function of the MHD stabilization capabilities of the minimum-B cells in the tandem (plugs or "A" cells), and the value chosen is still an estimate.

We assumed 100% alpha particle thermalization and included the hot alpha dilution of the central cell fuel, but neglected the effects of any thermal

alpha buildup. This is, of course, an optimistic assumption, and we must develop a realistic treatment of alpha particle transport in tandem mirrors. Logan did show[4] that a thermal alpha density fraction of 0.1 can be accommodated without a severe performance penalty.

The Power Balance-Power Density Tradeoff

Tradeoffs between power balance and power density are inherent to the tandem mirror reactors we have studied. Better power balance (e.g., lower ratio of power recirculated to gross power produced) can always be achieved at the expense of power density (e.g., power produced per unit volume or mass), and vice-versa. In our first tandem mirror parametric studies,[3] these tradeoffs were present but somewhat hidden because we attempted to optimize the design for the minimum cost of net electric power. Although we believe that approach to be valid, the results are sensitive to the rather large uncertainties in the efficiency and cost of the various reactor systems.

In our present work, we have chosen to present our results in a more general power balance vs power density format. The advantage of this format is that it permits after-the-fact tradeoff evaluations.

For the presentation of our results, we had to choose appropriate figures of merit for power balance and power density. We did not choose the recirculating power fraction as the power balance figure of merit because such results are then valid for only a unique set of component efficiencies. Instead, we chose the basic plasma performance quantity, Q, defined as the fusion power (17.6 MeV per DT fusion) divided by the trapped injection power from all external sources. For the power density figure of merit, we have chosen the first wall fusion neutron loading (Γ_n, in MW/m^2), but we have

also considered the variation of a volume-averaged neutron loading defined as

$$\bar{\Gamma} \equiv \Gamma \left(\frac{r_{fw}}{r_{fw} + t/2} \right)$$

where r_{fw} is the first wall radius and t is the thickness of the annular central cell (blanket, shield, and magnet). We have taken t = 2.0 m as typical. $\bar{\Gamma}$ is directly proportional to the fusion power per unit volume of central cell material. Although Γ is the more widely quoted parameter and is important for first wall life considerations, $\bar{\Gamma}$ is probably a better measure of the utilization of reactor capital investment. Note in Table 2 how $\bar{\Gamma}/\Gamma$ decreases with decreasing first wall radius. If two cases have the same Q and Γ, we should choose the case with larger first wall radius to maximize $\bar{\Gamma}$.

r_{fw}	$\bar{\Gamma}/\Gamma$ for t = 2 m
4 m	0.80
3	0.75
2	0.67
1	0.50
0.5	0.33

Table 2.
Volume-averaged wall loading as a function of first wall radius.

In summary, we will present our results as Q vs Γ curves, but will also comment on the variation of $\bar{\Gamma}$ where appropriate.

Some Initial Results

First, we considered TMR designs without "A" cells and with no direct electron heating. Given the plasma model and the constraints as discussed above, the three remaining independent variables are the neutral beam injection engery E_{inj}, the desired central cell ion temperature T_c, and the central cell magnetic field strength B_c.

Figure 1 shows Q vs Γ curves for various values of T_c at E_{inj} = 1200 keV and for T_c = 30 keV at E_{inj} = 800 keV. B_c increases from left to right along the curves. We see that the performance is strongly dependent on the injection energy: at constant Γ, Q drops by a factor of 2 if the injection energy is decreased from 1200 to 800 keV. If the injection energy is lowered to 600 keV, there is no solution, that is, the desired central cell ion temperature cannot be attained. This sensitivity to injection energy was the reason for specifying 1200 keV injection in our preliminary design.[3] Note that the various T_c curves on Fig. 1 are quite close together, indicating a shallow optimum for $T_c \approx 25$ keV. Because of the shallowness of this optimum, we calculated the results of the next three sections for a constant T_c, namely 30 keV. Then, we again consider the optimization of this variable.

Figure 1 shows the basic power balance-power density tradeoff: higher Q can be achieved at lower Γ, and vice-versa. Unfortunately, the performance curves are quite low: even with 1200 keV injection, Q = 5 can be obtained only at Γ less than 0.5 MW/m2; $\Gamma > 1$ MW/m2 can be obtained only with $Q < 3$. Clearly, improvements are necessary.

The "A" Cell

Next, we considered the effect of "A" cells in reducing the required injection energy. The "A" cell is an auxiliary plasma cell placed at each end of the tandem mirror, outside the plug cell. The purpose of the "A" cell is to reduce the outward potential drop of the plug plasma and thus improve the confinement of the plug plasma. Figure 2 shows the loss boundaries in velocity space for plug ions for the case without "A" cells. ϕ_c is the inward potential drop from the plug plasma, $\phi_e + \phi_c$ is the outward potential drop, and R_p is the plug plasma mirror ratio. Note the asymmetric plasma potential cutoffs. Plug confinement is primarily limited by the outward loss rate, especially in the usual circumstance of drag-dominated plugs, where the ion trajectory remains near the $v_\parallel$ axis. The presence of an "A" cell lowers the outside loss boundary; if the "A" cell density is maintained equal to the central cell density, then the loss boundaries become symmetric. This limiting case is the one we have considered in our parametric studies.

Because of the much lower density in the "A" cell than in the plug, the required injection power into the "A" cell can be almost negligible compared to the plug injection if the "A" cell mirror ratio and injection energy are wisely chosen. The "A" cell cases to be discussed next did not include a calculation of the "A" cell power requirement and therefore are slightly optimistic. (A following discussion will characterize the "A" cell itself and demonstrate that the required injection power can indeed be very small.)

Figure 3 shows Q vs Γ curves for tandem mirror reactors with "A" cells, T_c = 30 keV and E_{inj} = 1200, 800, and 600 keV. Comparing Fig. 3 with Fig. 1 indicates that adding "A" cells allows reducing the plug injection energy by 1/4 to 1/3 (i.e., 800 keV to 600, 1200 to 800) with no loss in performance. If, instead, the plug injection energy is held at 1200 keV, the performance improves to yield Q = 6.5 at Γ = 0.5 MW/m^2 and Q = 4.1 at Γ = 1.0.

The "A" cell calculations which were added to the physics model require as input the injection energy, vacuum mirror ratio, and β for the "A" cell. Then the Logan/Rensink plug model is used to calculate the required magnetic field strength and injection power for the "A" cell. Figure 4 shows the range of possible "A" cell parameters for a particular case where the plug injection power was 280 MW and the "A" cell potential drop was 320 keV. (This case does not match any of the calculations of Fig. 3, and is presented here only for illustrative purposes.) The "A" cell β was held constant at 0.7 (short-fat approximation). Note that P_A, the required injection power to both "A" cells, decreases with increasing "A" cell vacuum mirror ratio, R_A, and the injection energy. P_A can be reduced to 10% of the plug injection power for a range of parameters from $R_A = 2.25$ and an injection energy of 320 keV (equal to the potential drop) to $R_A = 1.5$ and an injection energy of 580 keV. The higher mirror ratio cases allow somewhat lower "A" cell central magnetic field strengths, but as shown in Fig. 4, the field strengths at the on-axis mirror point increase with mirror ratio.

We conclude that "A" cell parameters can be chosen so that the net benefit is appreciable, and that the benefit can be realized either as a reduction in plug injection energy, or improved performance (higher Q vs Γ curve), or both. However, we would like to raise the Q vs Γ curve still higher than seems possible with just "A" cells.

Direct Electron Heating in the Central Cell

In all of the cases described so far, the tandem mirror electrons are heated by collisions with central cell alpha particles and the high energy plug ions. It was recognized in our preliminary design study[3] that directly heating the electrons by some means could lower the required plug injection energy and improve performance. We have now investigated the

effects of electron heating more thoroughly. In this section, we assume that there is only one electron temperature throughout the tandem mirror, which is roughly consistent with the application of the electron heating in the central cell. (In a later, section we will consider the effects of significantly different electron temperatures which can result from the application of electron heating in the plugs.) Electron heating in the central cell may be technologically easier than electron heating in the plugs. Electron cyclotron heating (ECH) in the central cell could be done at the microwave frequency of gyrotrons presently under development (110 GHz), whereas ECH in the high field plugs would require higher frequencies. Physical access is also greater in the central cell. Another possibility for electron heating--axial injection of a relativistic electron beam--would probably heat mostly the central cell electrons.

As an independent variable specifying the amount of direct electron heating, we define f_{aux}, the ratio of direct electron heating to neutral beam injection power. Figure 5 shows the effect of adding direct electron heating to the central cell of tandem reactors with T_c = 30 keV, "A" cells, and 600 keV plug injection energy. We see a big improvement in performance as electron heating is added. There is a broad optimum in the amount of electron heating: virtually identical Q vs Γ curves result for f_{aux} = 3 to 5. The f_{aux} = 2 curve is definitely lower, as is f_{aux} = 10 curve. The choice from the broad optimum in f_{aux} could be made to favor the less expensive or more efficient heating method. Lacking that information, we would tentatively choose the case with lowest f_{aux} because it is the shortest, fattest machine and has the largest volume-averaged wall loading (see Fig. 6). The fattest machine also has the best prospect for DCLC stability of the plugs.

Next, we investigated direct electron heating in the central cell for reactors with T_c = 30 keV, "A" cells, and different plug injection energies. The energies considered were 200, 400, and 1200 keV. In each case, we found Q vs $\bar{\Gamma}$ curves qualitatively the same as that for 600 keV. In each case, there was a broad optimum in f_{aux}, and we selected the low end of the optimum because of higher $\bar{\Gamma}$. Figure 7 shows only the maximum performance curves for the various injection energies.

The optimum fraction of direct electron heating decreases with increasing injection energy. Thus, the optimum value of f_{aux} is 7 for 200 keV injection (7/8 of the total power input is direct electron heating), and only 1 for 1200 keV injection (1/2 of the total is direct electron heating).

Figure 7 shows that, given the optimum amount of direct electron heating at each injection energy, there is a broad optimum in injection energy. The 400 keV and 600 keV performance curves are nearly identical. The 200 keV and 1200 keV performance curves are lower, but by less than 10%.

The Effect of Different Magnetic Field Strengths

We took the 600 keV case of Fig. 7 at $\bar{\Gamma}$ = 1 MW/m^2 and investigated the effect of varying all of the magnetic field strengths proportionally. The result is a constant Q = 5.3, but as the fields are reduced, the central cell length increases and the wall loading decreases. The results are shown in Table 3.

B_{OP}	B_{max}		Γ	L_c
	$\eta_{coil} = 0.75$	$\eta_{coil} = 0.84$		
11.9 T	19	17 T	1.3 MW/m^2	210m
10.6 (base case)	17	15	0.97	240
10.0	16	14	0.83	260
8.75	14	13	0.59	320
7.5	12	11	0.39	390

Table 3. The effect of magnetic field strengih.

A Careful Reoptimization

Returning to the 400 and 600 keV curves of Fig. 7, we performed a careful reoptimization at $\Gamma = 1$ MW/m^2 to ensure that we had found the maximum Q. The primary reason for performing the reoptimization was to confirm that our early choice of $T_c = 30$ keV (based on the initial results of Fig. 1) was near optimum. To perform the reoptimzation, we used the new controller program to exercise the physics model.

For these calculations, we included the details of the "A" cell performance. In order to obtain a small injection power for the "A" cell, we chose an "A" cell mirror ratio of 1.5 and an injection energy equal to the plug injection energy. We also compared our resulting plug parameters to those required by our DCLC stability criterion.

In addition to the usual constraints on β values, plug magnetic field strengths, and fusion power output, we added the injection energy and $\Gamma = 1$ MW/m^2. The controller then varied B_c, T_c, and f_{aux} to maximize Q. Actually, only two of these variables are independent; the third is determined by the constraints. Pertinent results for the two injection energies are shown in Table 4.

E_{inj}		400	600
Max Q at $\Gamma = 1$ MW/m^2		5.2	5.2
$\bar{\Gamma}$		0.56	0.60
r_p/ρ_i	actual	31	34
	predicted lower limit for DCLC stability.	56	45

Table 4.

Optimized cases with "A" cells and direct electron heating of the central cell. Deuterium plugs.

We see again that the two injection energies give identical Q values at the same Γ, just as the two curves of Fig. 7 were identical. The Q values are slightly lower than in Fig. 7 because of the "A" cell power requirement. The 600 keV case is somewhat shorter and fatter, resulting in a higher $\bar{\Gamma}$, but the advantage is not great. We would choose the 400 keV case for its lower neutral beam injection energy except for the pessimistic prediction concerning DCLC stability of the plugs. Using our preliminary model for DCLC stability, we predict that both of these cases are unstable, but the 400 keV case is considerably further from meeting the criterion. The ratio of actual r_p/ρ_i to the predicted requirement is 0.76 for the 600 keV case and 0.55 for the 400 keV case.

In an attempt to relieve the DCLC stability problem without severely penalizing performance, we next considered hydrogen injection for the plugs. (All of our calculations to this point have assumed deuterium.) For DCLC stability, there is a twofold advantage to hydrogen: at the same energy and field, the gyro radius is reduced, thus increasing the actual r_p/ρ_i; and the required r_p/ρ_i is reduced. Another advantage to hydrogen is a reduced fusion neutron source in the plugs, which will ease the problems of magnet shielding and neutral beam hardening. Against these advantages must be weighed the reduced confinement for hydrogen, which will lower the achieveable Q. Table 5 gives the pertinent results for the optimized 400 keV case with hydrogen plugs.

E_{inj}		400
max Q at Γ = 1 MW/m^2		4.9
$\bar{\Gamma}$		0.51
r_p/ρ_i	actual	38
	predicted lower limit for DCLC stability	41

Table 5.

Optimized case with "A" cell and direct electron heating of the central cell. Hydrogen plugs.

Compared to the 400 keV of Table 4, we see that Q and $\bar{\Gamma}$ are both slightly reduced. But there is a large gain in the predicted DCLC stability: the ratio of actual r_p/ρ_i to the predicted requirement is 0.93. Because of the uncertain accuracy of our preliminary stability model, we take this case to be close enough and choose it as our base case for electron heating in the central cell. A list of parameters is given in Table 6.

Central Cell	Plug	"A" Cell
B_c = 2.5 T	B_{0p} = 10.6 T	B_{0A} = 6.0 T
β = 0.7	R_{vac} = 1.2	R_{vac} = 1.5
α heating fraction = 1.0	B_{mirror} = 12.7 T	B_{mirror} = 9.0 T
r_c = 0.72 m	β = 1.0	β = 0.7
r_{fw} = 1.1 m	E_{inj} = 400 keV	E_{inj} = 400 keV
L_c = 360 m	r_p = 0.37 m	r_A = 0.43 m
T_e = 52 keV	r_p/ρ_i = 41	E_A = 640 keV
T_c = 33 keV	T_e = 52 keV	ϕ_A = 290 keV
ϕ_c = 89 keV	E_p = 510 keV	n_A = 9.9 x 10^{13} cm^{-3}
n_c = 9.9 x 10^{13} cm^{-3}	ϕ_p = 89 keV	Neutral beam power = 4 MW (both "A" cells)
P_{fus} = 3000 MW	n_p = 5.5 x 10^{14} cm^{-3}	
Γ = 1.0 MW/m^2	Neutral Beam Power = 90 MW (both plugs)	
$\bar{\Gamma}$ = 0.51 MW/m^2		

electron heating power = 510 MW

$$Q = \frac{3000}{510 + 90 + 4} = 4.9$$

Table 6.

Optimized TMR with "A" cells and electron heating in the central cell. Hydrogen Plugs.

The central cell has a first wall radius of 1.1 m and a length of 360 m. The solenoid magnetic field strength is 2.5 T. The fusion power is 3000 MW, giving a first wall neutron loading of 1.0 MW/m^2 and a volume-averaged wall loading (over an assumed 2 m thickness) of 0.51 MW/m^2. The central cell requires 510 MW of electron heating.

The plug has a central magnetic field of 10.6 T, an on-axis mirror field of 12.7 T, and an estimated maximum conductor magnetic field of 15 to 17 T, depending on whether the plug is an axisymmetric mirror or minimum-B. Each plug requires the injection of 45 MW of 400 keV hydrogen (110 A).

The "A" cell has a central magnetic field of 6.0 T and an on-axis mirror field of 9.0 T. Each "A" cell requires the injection of 2 MW of 400 keV hydrogen (5 A).

Direct Electron Heating in the Plugs

In this section, we specify that the direct electron heating be applied in the plugs, and use the latest physics model which incorporates two electron temperatures--one for the trapped plug electrons and one for the passing central cell electrons. Electron heating in the plugs can result in a higher electron temperature there, which in turn enhances the confinement in the central cell (because the confining potential is proportional to the plug electron temperature and the log of the plug-to-central cell density ratio).

We have used the controller program to maximize Q under the usual constraints on β values, plug magnetic field strengths, fusion power, and several injection energies and first wall neutron loadings. Because of our previous experience with the DCLC stability criterion, we investigated both deuterium and hydrogen plugs, expecting the hydrogen cases to satisfy the stability criterion at a slight penalty in Q (as we found for those cases with direct electron heating in the central cell). A pleasant surprise was the Q

turned out to be significantly higher for the hydrogen cases, by as much as 50%. We now understand the reason for this improvement: At constant fusion power, switching to hydrogen plugs results in a decrease in both plug confinement and plug volume, and the net effect on Q is small and negative if the electron heating is applied to the central cell. However, in the case of plug electron heating, the reduced plug volume results in a higher plug electron temperature, which linearly increases the central cell confinement, and hence Q.

Our calculations for maximum performance as a function of injection energy show almost constant Q vs Γ curves for injection energies between 300 and 400 keV. However, if we go below 350 keV, we begin to violate the DCLC stability criterion for hydrogen. Thus, we have chosen 350 keV as the injection energy.

Figure 8 shows the maximum Q vs Γ curve for 350 keV injection energy. The performance varies from Q = 16 at Γ = 1 MW/m^2 to Q = 7.5 at Γ = 2 MW/m^2. For discussion purposes, we have chosen the design with Γ = 1.3 MW/m^2, which has Q = 10.5. The reactor parameters are given in Table 7.

Central Cell	Plug	"A" Cell
B_c = 2.7 T	B_{0P} = 10.6 T	B_{0A} = 7.4 T
β = 0.7	R_{vac} = 1.2	R_{vac} = 1.5
α heating fraction = 1.0	B_{mirror} = 12.7 T	B_{mirror} = 11 T
r_c = 0.6 m	β = 1.0	β = 0.7
r_{fw} = 0.9 m	E_{inj} = 350 keV	E_{inj} = 400 keV
L_c = 320 m	r_p = 0.32 m	r_A = 0.34 m
T_e = 45 keV	r_p/ρ_i = 30	E_A = 780 keV
T_c = 40 keV	T_e = 80 keV	ϕ_A = 260 keV
ϕ_c = 100 keV	E_p = 620 keV	n_A = 1.2 x 10^{14} cm^{-3}
n_c = 1.2 x 10^{14} cm^{-3}	ϕ_p = 100 keV	Neutral beam power = 4 MW (both "A" cells)
P_{fus} = 3000 MW	n_p = 4.4 x 10^{14} cm^{-3}	
Γ = 1.3 MW/m^2	Neutral Beam Power = 34 MW (both plugs)	
$\bar{\Gamma}$ = 0.63 MW/m^2	electron heating power = 250 MW (both plugs)	

$$Q = \frac{3000}{250 + 33 + 4} = 10.5$$

Table 7.

Optimized TMR with "A" cells and electron heating in the plugs. Hydrogen Plugs.

The central cell has a first wall radius of 0.9 m and a length of 320 m. The solenoid magnetic field strength is 2.7 T. The fusion power is 3000 MW, giving a first wall neutron loading of 1.3 MW/m^2 and a volume-averaged wall loading (over an assumed 2 m thickness) of 0.65 MW/m^2.

The plug has a central magnetic field of 10.6 T, an on-axis mirror field of 12.7 T, and an estimated maximum conductor magnetic field of 15 to 17 T, depending on whether the plug is an axisymmetric mirror or minimum-B. Each plug requires the injection of 17 MW of 350 keV hydrogen (50 A) and 125 MW of electron heating.

The "A" cell has a central magnetic field of 7.4 T and an on-axis mirror field of 11 T. Each "A" cell requires the injection of 2 MW of 350 keV hydrogen (6 A).

In conclusion, this tandem mirror reactor with "A" cells and electron heating of the hydrogen plugs is the best performing, lowest technology case we have calculated without resorting to the newest idea involving thermal barriers. The thermal barrier concept is discussed in Ref. 1.

Technology Requirements

In this section, we discuss some of the technological features of the reactor cases discussed in the last two sections. We will emphasize the technology requirements for those cases presented in Tables 6 and 7.

Magnets. The proposed arrangement of the several magnets for the tandem mirror reactor is shown in Fig. 9. From left to right, the figure shows part of the central cell solenoid (actually, the central cell magnets will be discrete solenoids covering about 30% of the cylindrical surface), two solenoidal coils making up the plug cell, a cee-shaped transition coil, and a Yin Yang "A" cell. The plasma within the central cell and plug is of circular cross section; the transition coil distorts this to an elongated shape, so

that the similar effect in the minimum-B "A" cell is cancelled, and the plasma returns to a circular cross section at the center of the "A" cell. The coil set shown was designed for a reactor case very similar to that given in Table 6 (TMR with "A" cells and electron heating in the central cell). For the case given in Table 7 (TMR with "A" cells and electron heating in the plugs), the "A" cell coils would need some redesign. The bulk current density and magnetic field values are given in Table 8.

Central Cell	Transition
B_c = 2 T	j = 1525 A/cm^2
	$B_{max} \simeq$ 15 T
Plug	**"A" Cell**
j = 1800 A/cm^2	j = 1575 A/cm^2
B_{op} = 10.9 T	B_{OA} = 5.8 T
R_{vac} = 1.16	R_{vac} = 1.48
B_{mirror} = 12.6 T	B_{mirror} = 8.6 T
$B_{max} \simeq$ 15 T	$B_{max} \simeq$ 13 T

Table 8. Magnet parameters.

The mean radius of the plug coil is 2.2 m, and the separation gap is 1.8 m. The mean radius of the major arc of the Yin Yang "A" cell is 3.9 m. The coil set was sized to accommodate a plug plasma of radius 0.7 m and has space for 1 m of shielding in the plug and about 0.8 m in the "A" cell. Since the plug plasma of Table 6 has a radius of only 0.37 m, the coil set is somewhat oversized. Also, the shielding space is larger than necessary now that we

have changed to hydrogen plugs and "A" cells. As shown in Ref. 4, Fig. 6-3, the largest contribution to neutron production in a deuterium plug is plug D reacting with plug D and the second largest contribution is plug D reacting with central cell T (the density of which falls to zero at the center of the plug). Both of these contributions are absent with hydrogen plugs, and we are left with only central cell D reacting with central cell T. The quantitative assessment of this improvement and the resulting reduction in coil size will be a part of our future work.

An advantage of this coil arrangement is that the highest on-axis field, the plug field, is produced by circular coils. We have been able to limit the maximum conductor field of these coils to 15 T. The lower coil efficiency typical of Yin Yangs would have resulted in a maximum field of about 17 T for the same on-axis field. The use of simple mirror plugs is permissible in this design if the minimum-B "A" cells provide MHD stabilization for the entire tandem mirror system. Although the plasma pressure is lower in the "A" cell than in the plug (bad for stability), the radial well depth or "good curvature" is large. We are just completing a computational tool for assessing the MHD stability of multicell tandem mirrors, and our future coil designs will address the issue quantitatively.

One of our concerns with this preliminary coil design is the large size of the transition coil. The large size is a result of several constraints: our choice of a circular outer plug coil, our desire to avoid a local field minimum between the outer plug coil and the "A" cell, and our desire to limit the maximum conductor field to 15 T. Our future work will investigate the use of a non-circular outer plug coil--either a planar elliptical coil or possibly a cee-shaped coil. This change will reduce the demands on the transition coil in reshaping the flux bundle.

It should be pointed out that the number and shape of coils shown in Fig. 9 (but not the sizes, currents, and field strengths) are appropriate for a tandem mirror with a thermal barrier as discussed in Ref. 1. In this case, the Yin Yang becomes the main plug (at a lower field than before) and the simple mirror cell becomes the thermal barrier. No "A" cell is required.

Neutral Beam Injectors. Figures 10 and 11 show a neutral beam injector designed to deliver 24 MW of 400 keV H^0. For the reactor described in Table 6, two such injectors are needed at each end plug. For the reactor described in Table 7, one somewhat smaller unit at each end plug will suffice.

The injector consists of four parallel beam lines in which cesium double charge exchange cells form negative ions, and cesium vapor stripping cells convert about 60% of the negative ions into neutrals. The high energy neutrals go directly into the reactor while the positive and negative ions leaving the stripper are deflected into water cooled beam dumps.

Two bands of epoxy form part of the wall that separates the low pressure beam region from the outer SF_6 chamber at one atmosphere in which the high voltage power supplies are housed. The accel grids and electrostatic shields are supported by rods which pass through the epoxy and provide access for power and water cooling.

To design and construct this injector, five developments must be completed. First, a continuous source of predominantly atomic 1 keV H^+ is required. But this can be considered to be almost a by-product of the continuous, predominantly atomic 120 keV D^+ source needed for the positive ion beam program.

Second is a cesium vapor cell which acts as a pressure barrier to the gas flowing out of the ion source, but at the same time suffers a negligible loss of cesium. The plug nozzle which confines the cesium vapor path as it crosses

the ion beam is presently under development at Berkeley and Livermore. The cesium loss can be kept to a minimum by collecting the vapor in a flowing bed of sodium-cesium eutectic maintained at -20°C and by baffling the beam line with liquid nitrogen-cooled baffles.

The third development consists of a three dimensional computer code to evaluate grid designs and study beam optics. As the beam pulse length is increased and the beam power goes up, the exact beam contours must be determined to prevent excessive wall heating. This is required for both positive and negative ion beams.

One of the more serious causes of high voltage-vacuum insulation failure results from charges streaking across insulator surfaces. Whereas a charge concentration will distort the local field, a large electric field can drive the charges to move across the insulator surface. This results in local heating, outgassing and sometimes tracking. To mitigate this effect, the fourth development consists of a resistive coating to bleed the charges from high voltage insulator surfaces. Recent studies have shown that the coatings tried in the past enhanced the secondary emission coefficient at the insulator surface and thereby increased the charge buildup. Preliminary results indicate that very light metallic coatings are the most promising candidates.

The fifth development involves reliable arc suppressors to limit the damage that an occasional arc might cause. This development is also essential for continuous operation of positive ion beam lines. Arc snubbers used in the 120 keV, TFTR beam lines, isolate the fault and limit the arc to the energy stored between the arcing electrodes. Experience has shown that arcs limited to about 2 Joules are self-quenching and do little or no damage. Pre-injectors for high energy particle accelerators arc every several hours without serious damage after an entire year of operation. Thus, if the energy

stored between grids and electrostatic shields is so limited, arcs would become permissible, provided the beam is turned off to be reignited after the fault had cleared. Fortunately, the time constants of the reactor plasma is such that a beam interruption of 100 ms is permissible.

The injector design described here is an attempt to show how far we can go with little more than present day technology. The individual concepts that make up the five proposed developments are not new. Most of these developments will probably be completed within the next couple of years as part of the on-going positive ion program. Thus, we believe that our design represents a realistic model of an operating neutral beam injector.

Electron Heating. Direct electron heating is an important element in our improved tandem mirror designs. The reactor case given in Table 6 requires 510 MW of direct electron heating in the central cell, and the case given in Table 7 requires 125 MW in each plug cell.

The only specific technology we have considered for electron heating is electron cyclotron heating (ECH) by gyrotrons.[10] Other potentially viable technologies, such as relativistic electron beams, should also be considered.

For the central cell-heated reactor case given in Table 6, the electron cyclotron frequency, ω_{ce}, is 70 GHz at the central cell vacuum field value of 2.5 T. The plasma frequency ω_{pe} at the central cell density is 89 GHz. Since we require $\omega_{pe} < \omega_{ce}$ for efficient microwave absorption in the plasma, we must apply the ECH in the transition region between the central cell and plug cell where $B > 2.5$ T. A possible choice is the location where $B = 3.9$ T, $\omega_{ce} = 110$ GHz and $\omega_{pe}/\omega_{ce} = 0.8$. The Department of Energy microwave source development program is presently focused on the development of a 200 kW continuously operating 110 GHz gyrotron device. Although such devices could be applied directly to our reactor, the large number of devices required (2500) points to the desirability of increased unit size. Based on

an estimated first wall launch power density of 10 kW/cm^2, we would require 2.6 m^2 of launch area at each end of the central cell. The first wall area is 6.9 m^2 per m of length and the gap between the last central cell coil and the plug coil is 3.8 m for the magnet design shown in Fig. 9, giving a total wall area in the transition region of 26 m^2. Thus, we need roughly 10% of the first wall area in the transition region for ECH launching.

For the plug-heated reactor case given in Table 7, ω_{ce} is 300 GHz at the plug central vacuum field value of 10.6 T. The plasma frequency ω_{pe} at the plug density is 190 GHz; so $\omega_{pe}/\omega_{ce} = 0.6$, an acceptable value for microwave absorption. However, such ECH heating will require microwave sources not now under development. On the positive side, only half as much ECH power must be launched into each plug as was required for each transition region for the previous case. If a launch power density of 10 kW/cm^2 is achievable at this frequency, we would require 1.3 m^2 of launch area in each plug, which is 11% of the area of a cylindrical surface 1 m in radius and of length 1.8 m, the gap distance between the two plug coils of Fig. 9.

We should point out that plug ECH heating in conjunction with the the new thermal barrier concept (see Table 1 and also Ref. 1) will be easier because the power required is much reduced, and the reduced plug magnetic field strength will lower the required microwave frequency.

A high efficiency for ECH microwave power production is desirable for our reactor applications. A single cavity 28 GHz pulsed gyrotron (Varian) has exhibited 37% efficiency without electron beam energy recovery. With a depressed collector for beam energy recovery, 50% efficiency should be attainable. Thermal recovery of the deposited heat at 33% efficiency could raise the overall efficiency to 67%, about equal to our estimated efficiency for negative ion type neutral beam injectors.

Mechanical Design of the Central Cell. As we have now seen, tandem mirror reactor design always involves tradeoffs between power balance and power density. In order to obtain an economical high Q reactor, it is imperative to develop a fundamentally inexpensive design approach for the central cell.

Our preliminary central cell design[3] was massive and rather costly because of the use of high pressure helium coolant in pressure containers of non-ideal shape, and because of the scenario for maintenance (lateral transport of entire central cell "slices", weighing 600 tonne each, on permanently affixed motorized crawlers).

Two entirely new concepts have now been studied. The first employed flowing lithium in reactor-length pipes. Though economic to construct, it proved to be costly and time consuming to service and repair. The second approach uses cylindrical blanket pods arranged in triangular modules as shown in Fig. 12. The chief design features of this central cell are:

1. Permanent installation of the shield and central cell solenoid coils. Blanket maintenance never involves movement of these components. However, they are accessible for accident repair.
2. More efficient use of blanket material in cylindrical pod pressure vessels.
3. Mechanically simple and reliable service machinery.
    a) Service "car" inside the cylindrical first wall.
    b) Easy access for service "car" entry at both ends of the central cell.
    c) Simultaneous blanket service by two "cars" if necessary--one from either end of the central cell.
    d) Easy access to module coolant connection from outside the shield.
    e) Blanket modules weigh less than one tonne each.

4. Poured lead-cement shield for lowest possible cost.
5. Integrated shield case and solenoid coil winding form simplifies installation and lowers cost.
6. Lithium-oxide blanket neutron moderator and tritium breeder. This allows a thinner blanket since more lithium atoms are present in a given volume than for elemental lithium.
7. Pressurized helium coolant.
    a) Simple plumbing disconnects
    b) No corrosion
    c) No neutronic effects
    d) No MHD losses
    e) Modest circulating power
8. If desired, a graphite spectrum-shifter to lengthen first-wall service life.
    a) For the 1 MW/m^2 design, the first-wall life may be 20 years.
    b) Glove-on-fingers design is rugged and easy to install.

In summary, we believe that this design approach can yield a central cell which is fundamentally inexpensive, and thus will allow reactor optimization at high Q.

REFERENCES

1. D. E. Baldwin, B. G. Logan, T. K. Fowler, An Improved Tandem Mirror Fusion Reactor, Lawrence Livermore Laboratory, Rept. UCID 18156, April 1979.

2. F. H. Coensgen, TMX Major Project Proposal, Lawrence Livermore Laboratory, Rept. Prop-148, January 12, 1977.

3. R. W. Moir, et al., Preliminary Design Study of the Tandem Mirror Reactor (TMR), Lawrence Livermore Laboratory, Rept. UCRL-52302, July 15, 1977.

4. B. G. Logan, et al., Tandem Mirror Reactors, Lawrence Livermore Laboratory, Rept. UCRL 80644, June 29, 1978. Also, Proceedings of the Seventh International Conference on Plasma Physics and Controlled Nuclear Fusion Research, Innsbruck, Austria, August 1978.

5. K. Shaing, R. W. Conn, J. Kesner, Parametric Studies of Tandem Mirror Reactors, University of Wisconsin, Rept. UWFDM-267.

6. G. Logan and M. Rensink, "Comparison of an Analytic Model for Tandem Mirror Plugs with Fokker-Planck Calculations", Lawrence Livermore Laboratory, Internal memorandum, MFE/CP/78-181, April 24, 1978.

7. L. D. Pearlstein - personal communication.

8. B. G. Logan - personal communication.

9. J. A. Nelder and R. Mead, A Simplex Method for Function Minimization, Comput. J. 7, 308 (1965)

10. We gratefully acknowledge our consultation with Ray Dandl on the subject of ECH heating.

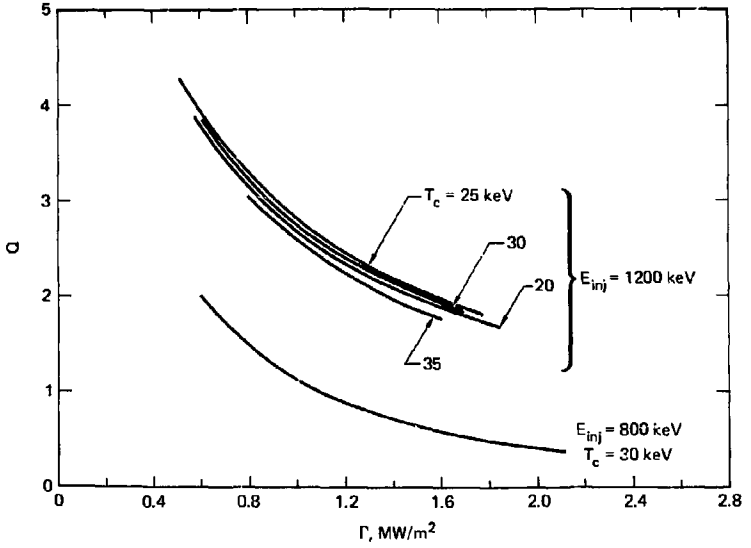

Figure 1. Performance of tandem mirror reactors without "A" cells or electron heating.

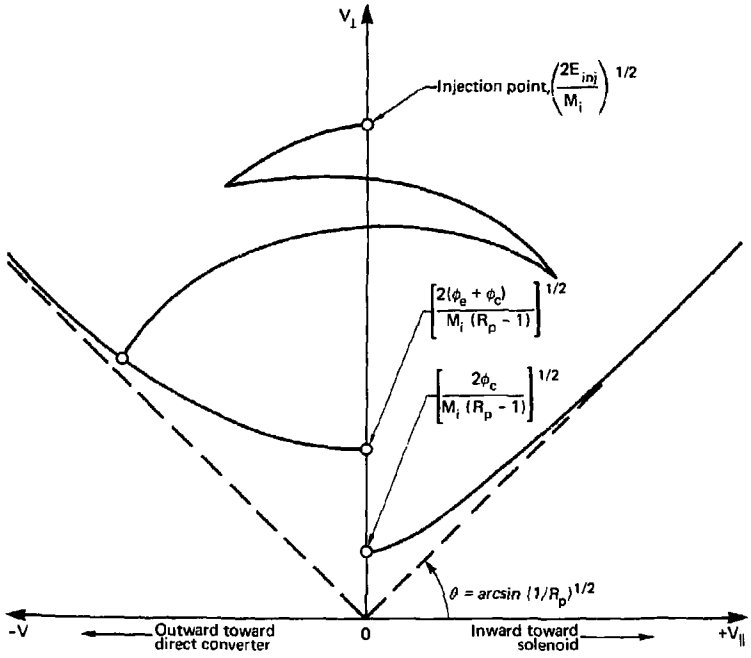
$V_\perp$
Injection point, $\left(\frac{2E_{inj}}{M_i}\right)^{1/2}$
$\left[\frac{2(\phi_e + \phi_c)}{M_i (R_p - 1)}\right]^{1/2}$
$\left[\frac{2\phi_c}{M_i (R_p - 1)}\right]^{1/2}$
$\theta = \arcsin (1/R_p)^{1/2}$
-V
Outward toward direct converter
0
Inward toward solenoid
$+V_\parallel$

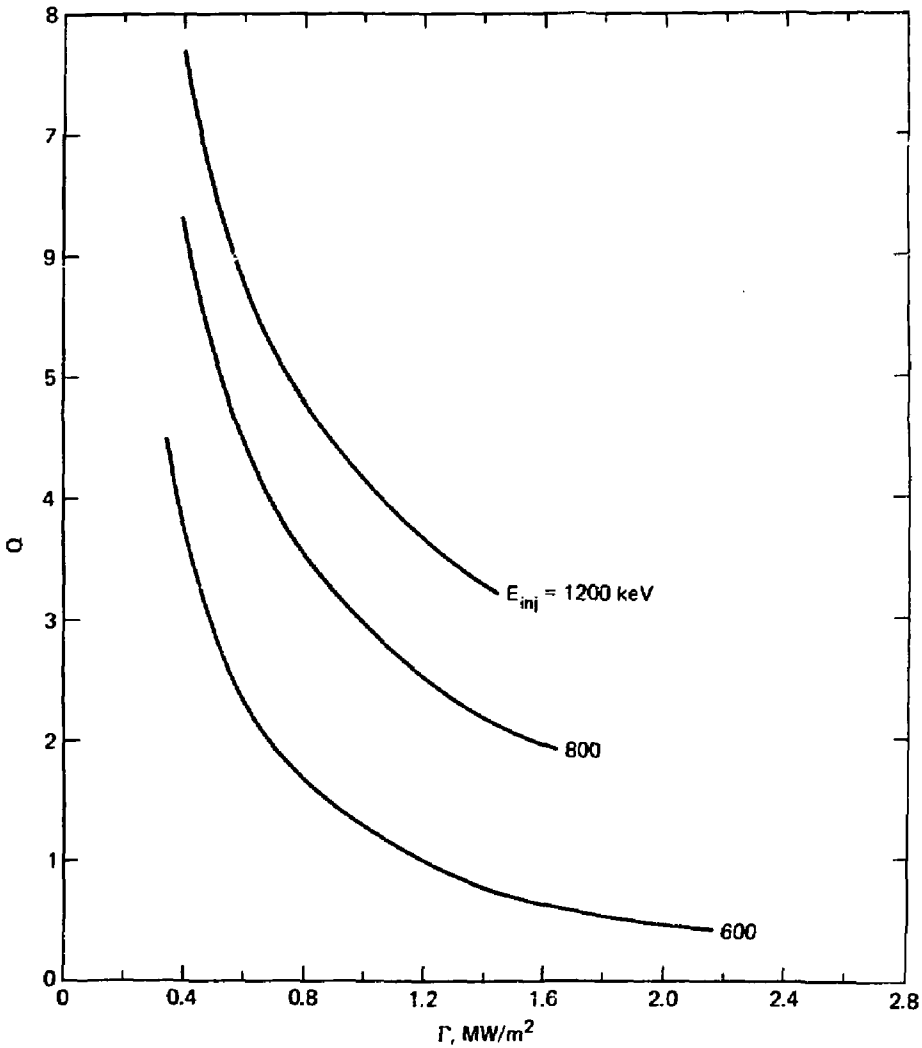

Figure 3. Performance of tandem mirror reactors with "A" cells.

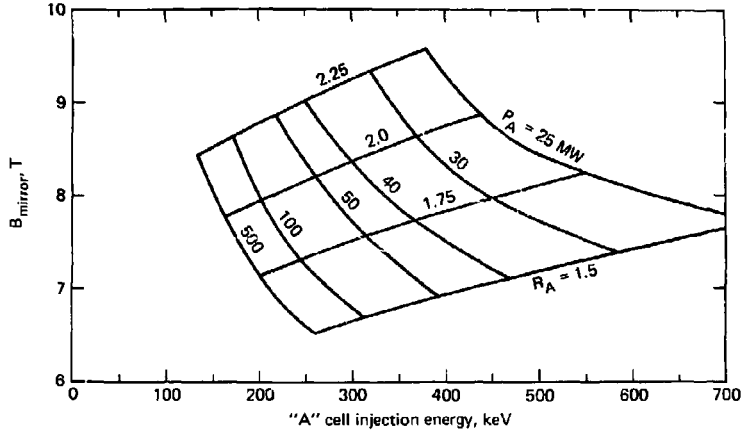

Figure 4. "A" cell parametrics.

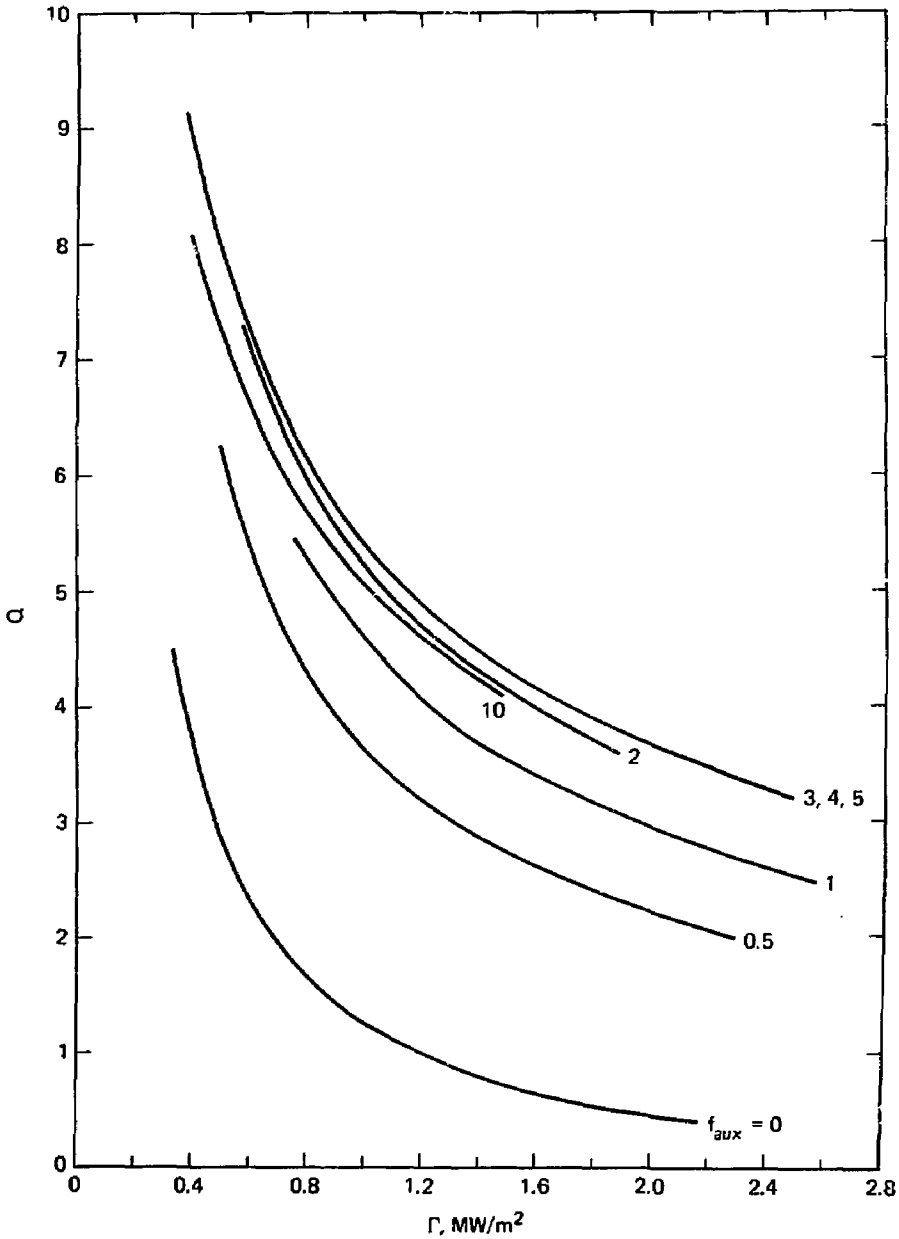

Figure 5. Performance of tandem mirror reactors with "A" cells and central cell electron heating. E_{inj} = 600 keV.

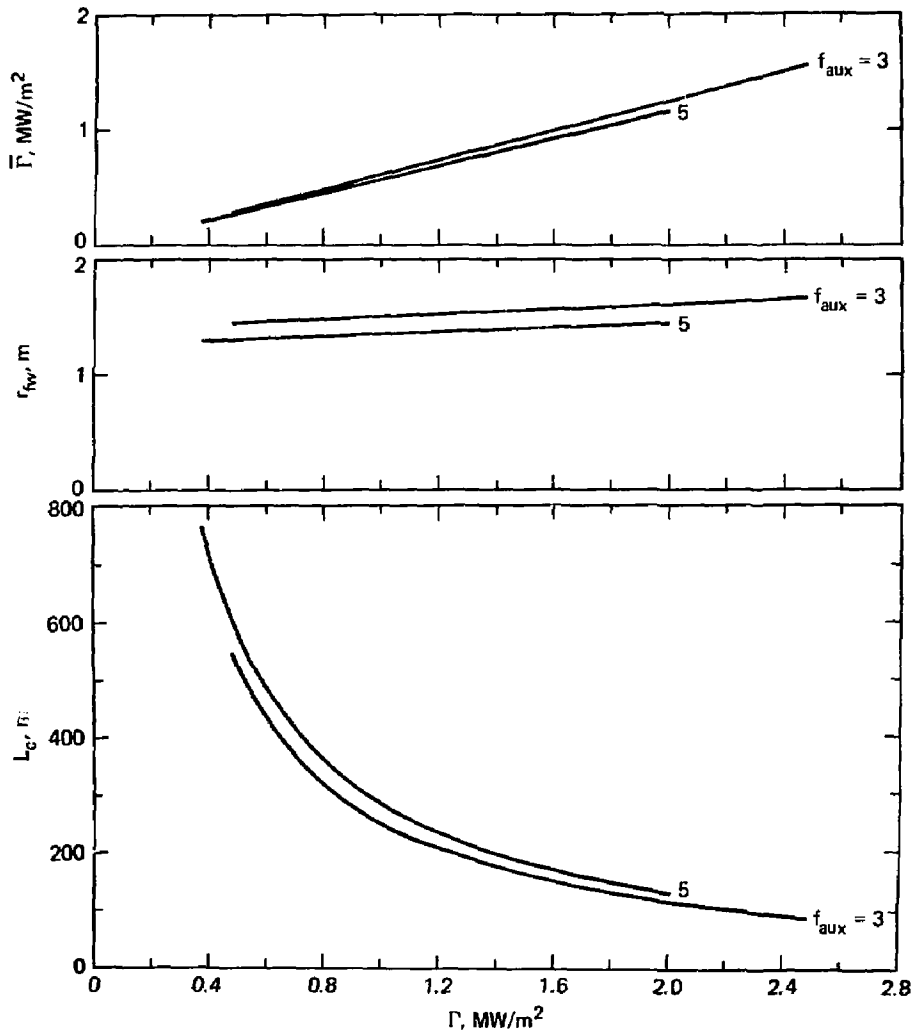

Figure 6. Characteristics of maximum performance designs from Fig. 5.

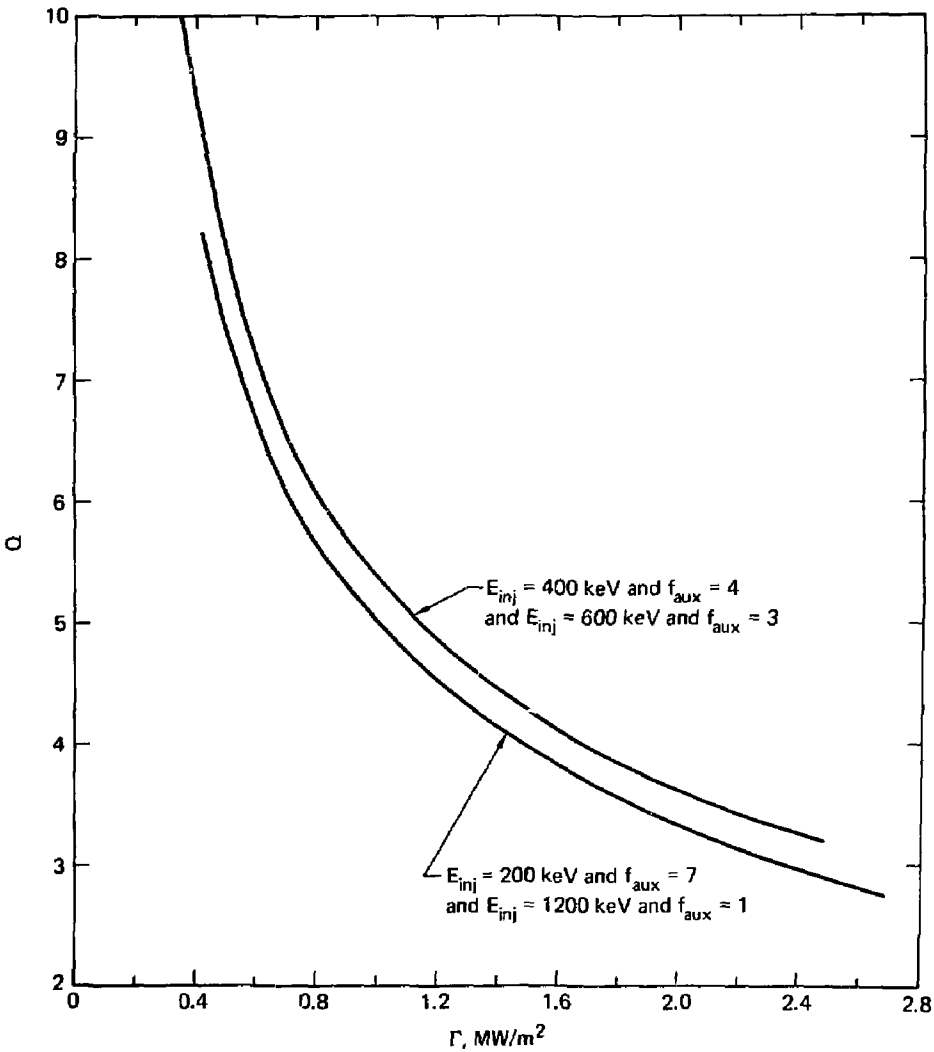

Figure 7. Maximum performance of tandem mirror reactors with "A" cells and central cell electron heating.

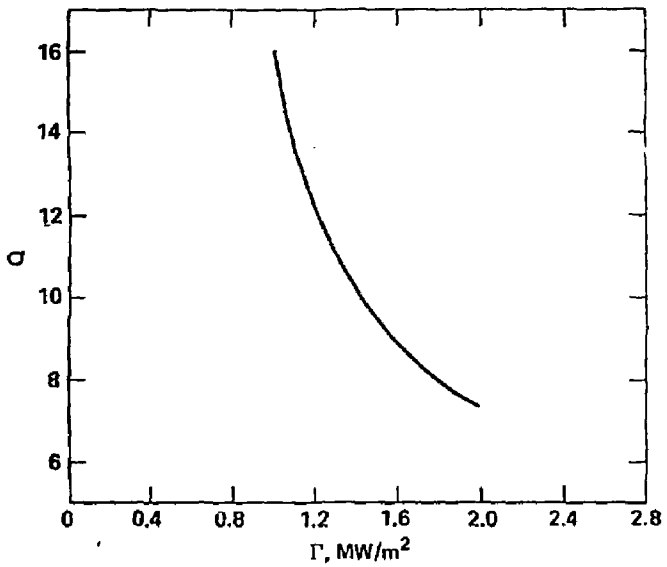

Figure 8. *Maximum performance* of tandem mirror reactors with "A" cells and plug electron heating. $E_{inj} \approx 350$ keV. Hydrogen plugs.

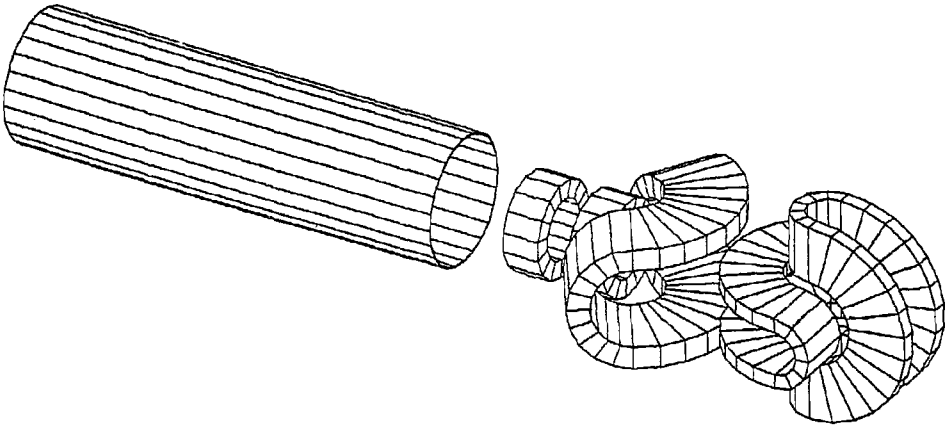

Figure 9. Tandem mirror reactor magnet arrangement showing simple mirror plug cell, cee-shaped transition coil, and Yin Yang "A" cell.

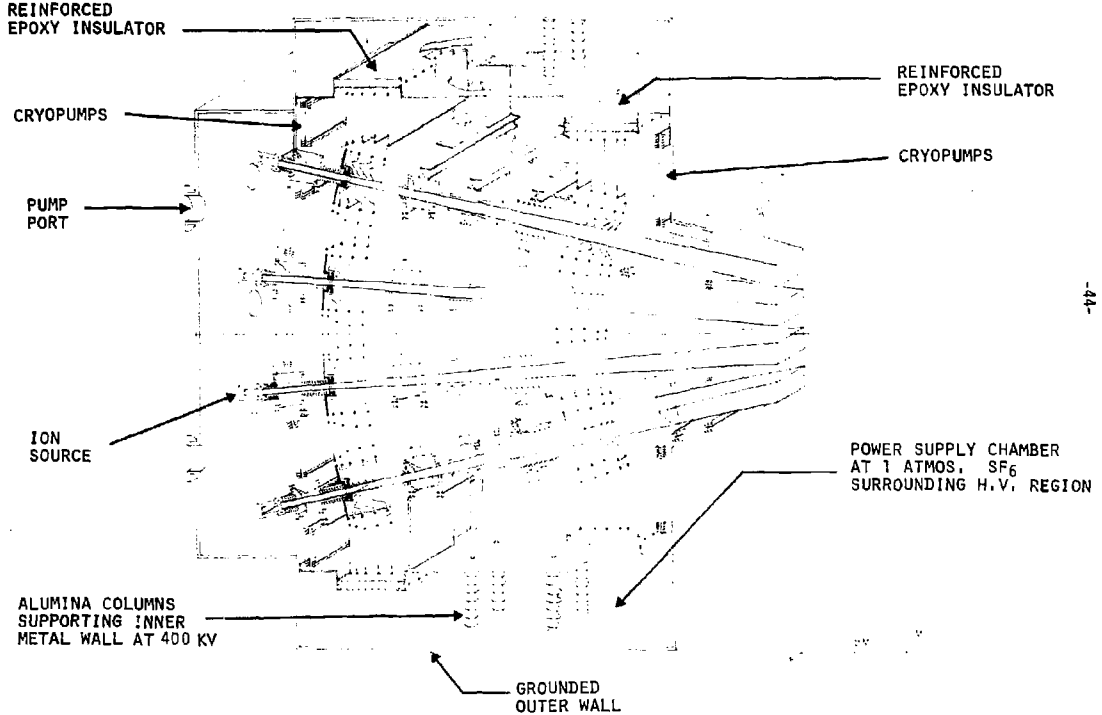
REINFORCED
EPOXY INSULATOR
CRYOPUMPS
PUMP
PORT
ION
SOURCE
ALUMINA COLUMNS
SUPPORTING INNER
METAL WALL AT 400 KV
REINFORCED
EPOXY INSULATOR
CRYOPUMPS
POWER SUPPLY CHAMBER
AT 1 ATMOS. SF_6
SURROUNDING H.V. REGION
GROUNDED
OUTER WALL

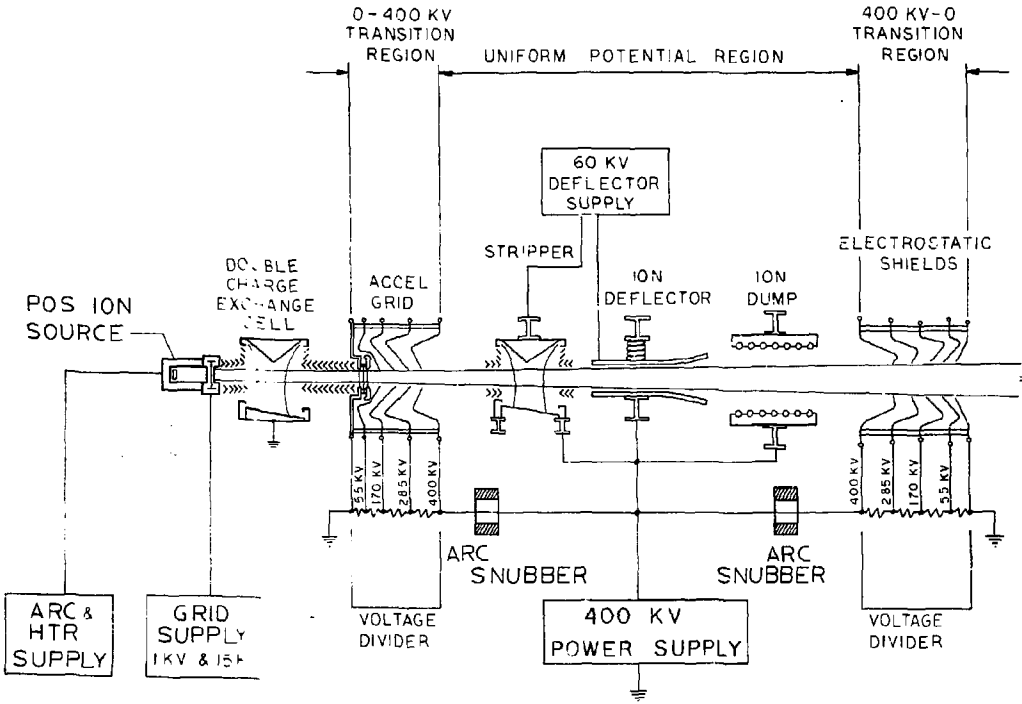

Figure 11. Schematic of the Neutral Beam Line.

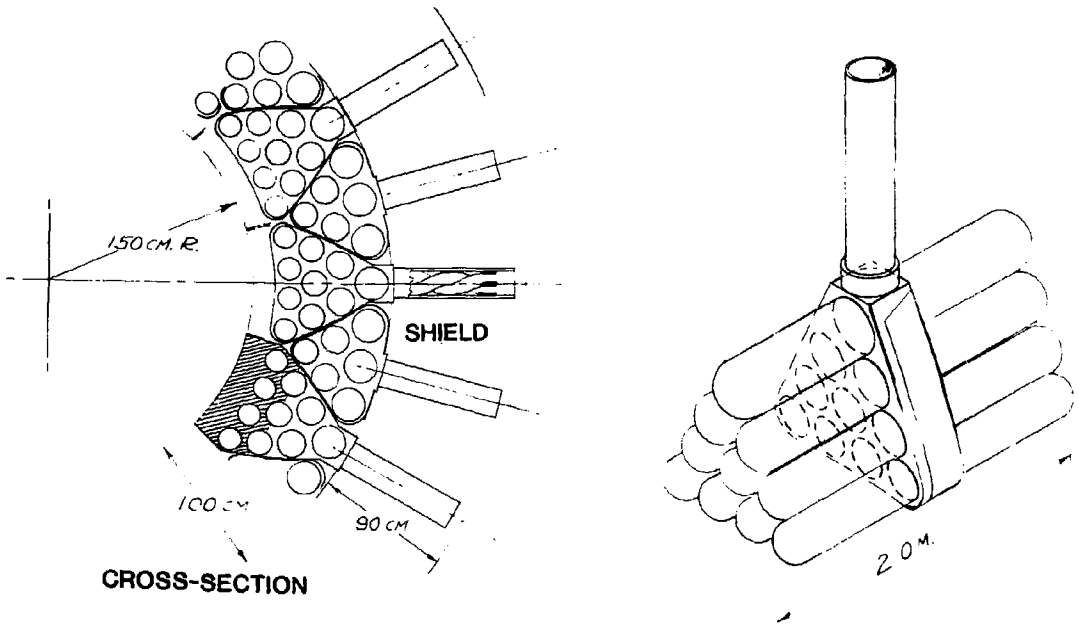

Figure 12. Cylindrical pod modular blanket design for tandem mirror reactor.